KEK-PREPRINT-92-34

Fermilab Library
0 1160 0009187 0

KEK Preprint 92-34
May 1992
H

12

1992

Dependence of Properties of SUSY Particles on the Minimal SUSY Model Parameters

T. TSUKAMOTO

ROUTE TO

NAME	LOCATION
Werner	318

RETURN TO FERMI LIBRARY

Talked at the 3rd JLC Workshop, KEK, Japan, Feb. 18-20, 1992.

National Laboratory for High Energy Physics, 1992

KEK Reports are available from:

Technical Information & Library
National Laboratory for High Energy Physics
1-1 Oho, Tsukuba-shi
Ibaraki-ken, 305
JAPAN

Phone:	0298-64-1171	
Telex:	3652-534	(Domestic)
	(0)3652-534	(International)
Fax:	0298-64-4604	
Cable:	KEKOHO	

Dependence of properties of SUSY particles
on the Minimal SUSY model parameters

T.Tsukamoto

National Laboratory for High Energy Physics (KEK), Ibaraki 305, Japan

Abstract

I present some general dependence of properties of SUSY particles on the Minimal SUSY model parameters for further simulation studies. Considered are masses, decay branching ratios and cross sections.

1 Introduction

SUSY model is one of the candidates which solve the naturalness problem and it becomes more attractive one as the LEP data shows that three couplings of SU(3) ⊗ SU(2) ⊗ U(1) can be unified at high energy with SUSY contents. Although there may be many SUSY models, the Minimal SUSY standard model (MSSM) with the framework of N=1 minimal supergravity(SUGRA) model is considered in this report. First I show dependence of SUSY particle masses on SUSY parameters, and then present results such as decay branching ratios and production cross sections for fixed SUSY particles masses. Finally I present some contours in SUSY parameters space and focus on $\tilde{\mu}$-pair production showing "clean" cross sections, i.e. $e^+e^- \to \tilde{\mu}_{L/R}\bar{\tilde{\mu}}_{L/R}$, and $\tilde{\mu} \to \mu\tilde{\chi}^0_1$ as a detectable channel to see how much cross section we keep by using "clean" mode.

2 Mass of SUSY particles

There are four(five) parameters to fix the considered SUSY model as follows; μ: Higgsino mass, M_3: gluino mass, tanβ: ratio of the two vacuum expectation values of Higgses and m_0: common scalar mass (and m_P:pseudo-scalar mass(=mass of

pseudo-scalar Higgs, which appears as decay products of SUSY particles in the following discussions)). (Although all of these are not independent in N=1 SUGRA, there are no problems in the following discussion.) We can know masses and couplings for interaction of SUSY particles with these parameters[1],[2] except for the Higgs particles and third generation sfermions on which radiative corrections have large effect. Mass of sfermions are calculated by solving the renormalization group equations and the results are

$$
\begin{aligned}
m_{\tilde{u}_L}{}^2 &= m_0{}^2 + 0.837M_3{}^2 + (\tfrac{1}{2} - \tfrac{2}{3}\sin^2\theta_W)m_Z{}^2\cos2\beta \\
m_{\tilde{d}_L}{}^2 &= m_0{}^2 + 0.837M_3{}^2 - (\tfrac{1}{2} - \tfrac{1}{3}\sin^2\theta_W)m_Z{}^2\cos2\beta \\
m_{\tilde{u}_R}{}^2 &= m_0{}^2 + 0.783M_3{}^2 + \tfrac{2}{3}\sin^2\theta_W m_Z{}^2\cos2\beta \\
m_{\tilde{d}_R}{}^2 &= m_0{}^2 + 0.777M_3{}^2 - \tfrac{1}{3}\sin^2\theta_W m_Z{}^2\cos2\beta \\
m_{\tilde{\nu}}{}^2 &= m_0{}^2 + 0.52M_\infty{}^2 - \tfrac{1}{2}m_Z{}^2\cos2\beta \\
m_{\tilde{l}_L}{}^2 &= m_0{}^2 + 0.52M_\infty{}^2 - (\tfrac{1}{2} - \sin^2\theta_W)m_Z{}^2\cos2\beta \\
m_{\tilde{l}_R}{}^2 &= m_0{}^2 + 0.1505M_\infty{}^2 - \sin^2\theta_W m_Z{}^2\cos2\beta
\end{aligned}
$$

where

$$\frac{M_3{}^2}{M_\infty{}^2} = 7.77 \quad (\text{with } \sin^2\theta_W = 0.232)$$

Mass of charginos and neutralinos and couplings for interactions are obtained by diagonalizing the mass matrices in the mass terms as

$$
\begin{aligned}
-\mathcal{L}_m &= (\bar{\tilde{W}}^-_R \bar{\tilde{H}}^-_{2R}) M_{(charge)} \begin{pmatrix} \tilde{W}^-_L \\ \tilde{H}^-_{1L} \end{pmatrix} + h.c. \\
&\quad + \frac{1}{2}(\tilde{B}^0_L \tilde{W}^0_L \tilde{H}^0_{1L} \tilde{H}^0_{2L}) M_{(neutral)} \begin{pmatrix} \tilde{B}^0_L \\ \tilde{W}^0_L \\ \tilde{H}^0_{1L} \\ \tilde{H}^0_{2L} \end{pmatrix} + h.c.
\end{aligned}
$$

with

$$M_{(charge)} = \begin{pmatrix} M_2 & \sqrt{2}m_W\cos\beta \\ \sqrt{2}m_W\sin\beta & \mu \end{pmatrix}$$

$$M_{(neutral)} = \begin{pmatrix} M_1 & 0 & -m_Z\sin\theta_W\cos\beta & m_Z\sin\theta_W\sin\beta \\ 0 & M_2 & m_Z\cos\theta_W\cos\beta & -m_Z\cos\theta_W\sin\beta \\ -m_Z\sin\theta_W\cos\beta & m_Z\cos\theta_W\cos\beta & 0 & -\mu \\ m_Z\sin\theta_W\sin\beta & -m_Z\cos\theta_W\sin\beta & -\mu & 0 \end{pmatrix}$$

$$M_2 = \frac{\alpha_e}{\alpha_s \sin^2\theta_W} M_3, \quad M_1 = \frac{5}{3}\tan^2\theta_W M_2$$

$M_{(charge)}$ can be diagonalized by two orthogonal matrices:

$$O_R M_{(charge)} O_L^T = diagonal,$$

with

$$O_{L,R} = \begin{pmatrix} \cos\phi_{L,R} & \sin\phi_{L,R} \\ -\sin\phi_{L,R} & \cos\phi_{L,R} \end{pmatrix}$$

$M_{(neutral)}$ can also be diagonalized by an orthogonal matrix:

$$O_N M_{(neutral)} O_N^T = \text{real diagonal},$$

and it is necessary to introduce a phase factor of i to make positive mass eigenstates if the above eigenvalues are negative:

$$U_N M_{(neutral)} U_N^T = \text{positive diagonal},$$

where $U_N = \Phi_N O_N$, and $(\Phi_N)_{ij} = \delta_{ij}\eta_i$ with

$$\eta_i = \begin{cases} 1 & \text{if the mass eigenvalue} \geq 0 \\ i & \text{if the mass eigenvalue} < 0 \end{cases}$$

Fig.1 shows dependence of sfermion masses on M_3 for four values of m_0=100, 200, 400GeV. One can see that squark masses are almost proportional to M_3, sleptons are lighter than squarks and are governed by m_0, and $\tilde{e_R}$ (and $\tilde{\mu_R}$) is the lightest sfermion except for a region of small M_3 values. Fig.2 shows dependence of charginos($\tilde{\chi}_i^{\pm}$) and neutralinos($\tilde{\chi}_i^0$) masses on M_3 for three μ values with tanβ=2. With large μ or M_3, $\tilde{\chi}_i^{\pm,0}$ are split into two groups, the lighter ($\tilde{\chi}_1^{\pm}$ and $\tilde{\chi}_{1,2}^0$) and the heavier ($\tilde{\chi}_2^{\pm}$, and $\tilde{\chi}_{3,4}^0$) and masses of heavier group become to be $\sim \mu$ when μ is large.

3 Decay branching ratios

Two body decays of SUSY particles are considered, which are

$$\tilde{f}_{L/R} \to f\tilde{\chi}_i^0$$
$$\tilde{f}_{1L/R} \to f_2\tilde{\chi}_i^-$$
$$\tilde{\chi}_i^- \to W^-/H^-\tilde{\chi}_j^0$$
$$\tilde{\chi}_i^- \to Z^0/h^0/H^0/P^0\tilde{\chi}_j^-$$

where $(f_1, f_2) = (\bar{u}, d)$, (d, u), (l, ν), $(\bar{\nu}, \bar{l})$, and H^-: charged Higgs, h^0: lighter Higgs, H^0: heavier Higgs and P^0:pseudo-scaler Higgs.

With five input parameters of μ, M_3, tanβ, m_0 and m_P, we can calculate the decay branching ratios for decay modes listed above assuming that other modes, such as three body decays, are negligible. Results are shown in Fig.3 as a function of M_3 with fixed other parameters shown in the figure, where the masses of SUSY particles are functions of M_3 as described in the previous chapter. Note the variety of branching ratios and almost one decay mode for $\tilde{e}_R$ ($\tilde{\mu}_R$) which will be discussed in the chapter 5.

4 Production cross sections

Considered processes are pair productions at e^+e^- collider such as

$$\begin{aligned} e^+e^- &\to \tilde{\chi}_1^-\tilde{\chi}_1^+ \\ &\to \tilde{\mu}_{L/R}\bar{\tilde{\mu}}_{L/R} \\ &\to \tilde{\nu}_\mu\bar{\tilde{\nu}}_\mu \\ &\to \tilde{e}_{L/R}\bar{\tilde{e}}_{L/R} \\ &\to \tilde{e}_L\bar{\tilde{e}}_R + h.c. \\ &\to \tilde{\nu}_e\bar{\tilde{\nu}}_e \end{aligned}$$

Fig.4 shows the cross sections for chargino pair production, where those corresponding to three cases of mixing angles($\phi_{L,R}$) for diagonalizing the mass matrix are plotted together with μ pair cross section. Although there are some dependence on mixing angles, this cross section is as large as μ pair's if $m_{\tilde{\chi}_1^-} < \sim$ 300GeV, which corresponds to the region of $M_3 < \sim$ 1000GeV as seen in Fig.3.

As there are only s-channel diagrams by γ/Z^0 exchange for $\tilde{\mu}$ pair and $\tilde{\nu}_\mu$ pair production, differential cross sections are proportional to $\sin^2\theta$ (θ is a polar angle with respect to e^- in e^+e^- CM system). For $\tilde{e}$ pair and $\tilde{\nu}_e$ pair production, there are t-channel diagrams where neutralinos or charginos are exchanged and so the differential cross sections have forward peaks. Note that there is a $\tilde{e}_L\bar{\tilde{e}}_R$ production process which is occurred by t-channel $\tilde{\chi}_i^0$ exchange and is absent in $\tilde{\mu}$ pair production. Fig.5 shows total cross sections for slepton pair production and Fig.6 shows differential cross sections for $\tilde{e}/\tilde{\nu}_e$ pair.

5 Dependence on SUSY model parameters

The simplest and cleanest mode in SUSY particles searches is pair production and their decays to an ordinary particle and the lightest SUSY particle (LSP) which is the lightest neutralino $\tilde{\chi}_1^0$ in general. But there is a problem how much of the SUSY parameter space is covered by this mode, as cross sections and decay branching ratios depend on the parameters.

As a simple example, in Fig.7 I show the contour of mass difference $\Delta M = m_{\tilde{\chi}_1^-} - m_W$ in the $M_3 - \mu$ plane with fixed other parameters which are same as in Fig.3 for $\tilde{\chi}_1^-$. The hatched region is $\Delta m > m_W$ where $\tilde{\chi}_1^-$ can decay into $W^-\tilde{\chi}_1^0$ (and decay branching ratio of $W^-\tilde{\chi}_1^0$ is 100% with other fixed parameters). We can search for $\tilde{\chi}_1^-$ with the cleanest mode in this parameter region, but in other region we should study final three body decay of $\tilde{\chi}_1^-$ which is familiar mode in e^+e^- experiments done so far.

Next I present the results of same analysis for $\tilde{\mu}_{L/R}$. Contours of mass differences $\Delta m = m_{\tilde{\mu}_{L/R}} - m_{\tilde{\chi}_1^0}$ are shown in Fig.8 and one can see that nearly equally spacing lines are drawn showing the fact that slepton mass is almost governed by m_0 as previously mentioned. Fig.9 shows contour plots for decay branching ratio of $\tilde{\mu}_{L/R} \to \mu\tilde{\chi}_1^0$ in the $M_3 - m_0$ plane and the $M_3 - \mu$ plane with other fixed parameters. It should be noted that $\tilde{\mu}_R$ decays mainly into $\mu\tilde{\chi}_1^0$ in almost all parameter region shown in the figure, but $\tilde{\mu}_L$ doesn't. Contour plots for the "clean" cross section, $\sigma(e^+e^- \to \tilde{\mu}_{L/R}\bar{\tilde{\mu}}_{L/R}) \cdot BR^2(\tilde{\mu}_{L/R} \to \mu\tilde{\chi}_1^0)$, are shown in Fig.10. We have large "clean" cross section for $\tilde{\mu}_R$ in wide parameter region but small for $\tilde{\mu}_L$ due to its decay branching ratio and mass($m_{\tilde{\mu}_L} > m_{\tilde{\mu}_R}$ in general), so we can access wider parameter region with $\tilde{\mu}_R$ than with $\tilde{\mu}_L$.

6 Summary and conclusions

Some MSSM parameters dependence of SUSY particles, such as masses, decay branching ratios and cross sections for pair production at e^+e^- colliders, are presented. The results show that $\tilde{\mu}_R$ ($\tilde{l}_R$ in general) or $\tilde{\chi}_1^-$ might be the first SUSY particle which can be observed in the "clean" mode, and especially wide parameter region can be covered by "clean" $\tilde{\mu}_R$ mode. In lower M_3 or μ region, three body decays of $\tilde{\chi}_1^-$

should be studied because $m_{\tilde{\chi}_1^-} - m_{\tilde{\chi}_1^0} < m_W$.

Next tasks are simulation studies for mass determinations of SUSY particles because SUSY model parameters can be deduced from masses in principle ($m_f = m_f(M_3, m_0, \tan\beta)$ and $m_{\tilde{\chi}_i^{-,0}} = m_{\tilde{\chi}_i^{-,0}}(M_3, \mu, \tan\beta)$), and would be very important to test the MSSM if SUSY particles were discovered.

Acknowledgement

I wish to thank Dr.K.Hikasa who prepared the private note of SUSY for experimentalists which is a basis for calculations presented in this report, and also thank Dr.K.Fujii for giving results of production cross sections for $\tilde{\chi}_1^-$.

References

[1] K.Hikasa, Supersymmetry Manual (private note, unpublished).

[2] For reviews, H.E.Haber and G.L.Kane, Phys. Rep. **117**,75(1985); H.Baer, A.Bartl, D.Karatas, W.Majerotto and X.Tata, MAD/PH/422.

Figure Captions

Figure 1: Mass dependence of sfermions on M_3 for m_0=100, 200 and 400GeV which one can know as approaching point when $M_3 \to 0$.

Figure 2: Mass dependence of charginos and neutralinos on M_3 for $\mu = m_W$(a), $5 \cdot m_W$(b) and $20 \cdot m_W$(c) with $\tan\beta = 2$.

Figure 3: Decay branching ratios of two body decay modes by neglecting decays into more than two bodies. (a)~(c) are for sleptons with (a): $\mu = 5 \cdot m_W$, $\tan\beta$=2, m_0=100GeV, (b): $\mu = 5 \cdot m_W$, $\tan\beta$=-2, m_0=100GeV and (c): $\mu = m_W$, $\tan\beta$=2, m_0=100GeV. (d) is for charginos.

Figure 4: Cross sections for chargino pair production with fixed chargino mass=100, 200, 300, 400GeV which can be identified by the position of the threshold, mixing angles $\phi_L = \phi_R$=0(solid), $\frac{\pi}{4}$(dot-dash), $\frac{\pi}{2}$(dash) and $m_{\tilde{e}}$=500GeV, together with μ-pair production(dot-dot-dash).

Figure 5: Cross sections for slepton pair production at $\sqrt{s}$=1TeV with $m_{l,\tilde{\nu}}$ = 250GeV, and M_3=1TeV, $\mu = 5 \cdot m_W$ and $\tan\beta$=2.

Figure 6: Differential cross sections for $\tilde{e}$ and $\tilde{\nu}_e$ at $\sqrt{s}$=1TeV with $m_{\tilde{e}} = m_{\tilde{\nu}}$ = 250GeV, and M_3=1TeV, $\mu = 5 \cdot m_W$ and $\tan\beta$=2.

Figure 7: Contour plot for mass difference: $\Delta m = m_{\tilde{\chi}_1^-} - m_{\tilde{\chi}_1^0}$ in the $M_3 - \mu$ plane. Hatched region shows $\Delta m > m_W$ where $\tilde{\chi}_1^-$ can decay into $W^-\tilde{\chi}_1^0$.

Figure 8: Contour plots for mass difference: $\Delta m = m_{\tilde{\mu}_{L/R}} - m_{\tilde{\chi}_1^0}$ in the $M_3 - m_0$ plane. Hatched is a region where LSP is not a neutral particle or $m^2{}_{\tilde{f}} < 0$.

Figure 9: Contour plots of decay branching ratio for $\tilde{\mu}_{L/R} \to \mu\tilde{\chi}_1^0$ in the $M_3 - m_0$ ((a),(b)) plane and the $M_3 - \mu$ plane ((c),(d)). Hatched is a region where LSP is not a neutral particle or $m^2{}_{\tilde{f}} < 0$.

Figure 10: Contour plots of cross section for "clean" $\tilde{\mu}_{L/R}$ mode: $e^+e^- \to \tilde{\mu}_{L/R}\bar{\tilde{\mu}}_{L/R}$, $\tilde{\mu}_{L/R} \to \mu\tilde{\chi}_1^0$. Hatched is a region where LSP is not a neutral particle or $m^2{}_{\tilde{f}} < 0$.

Fig.1

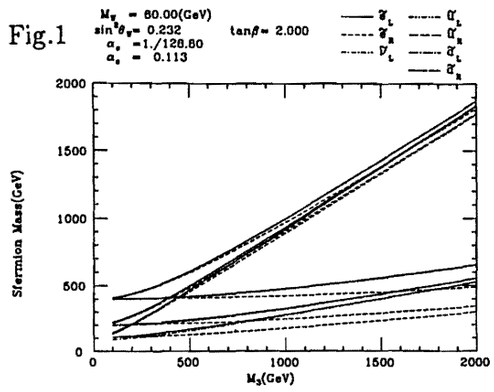

Fig.2(a)

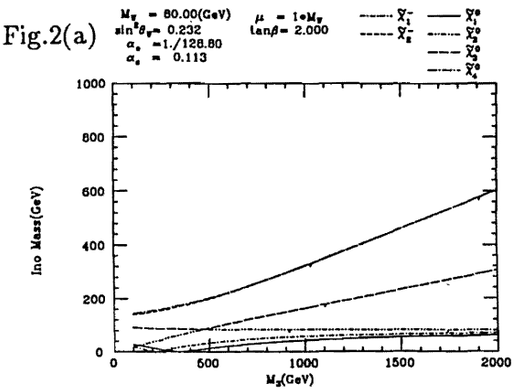

Fig.2(b)

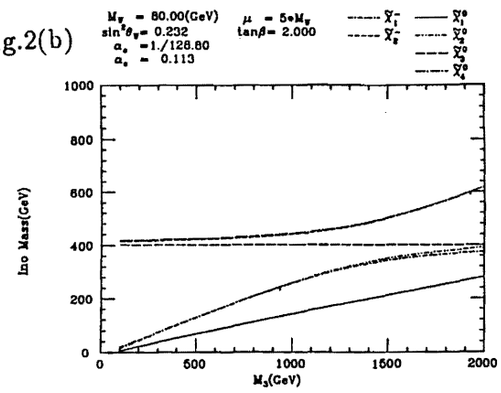

Fig.2(c)

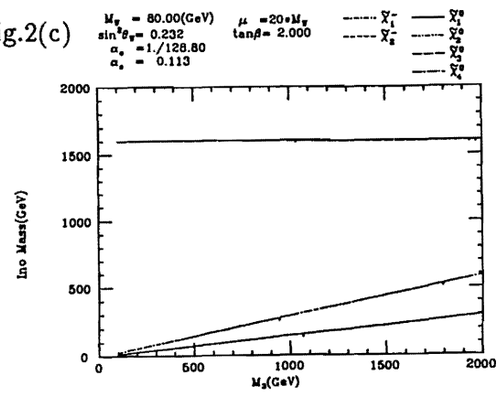

Fig.3(a)-2

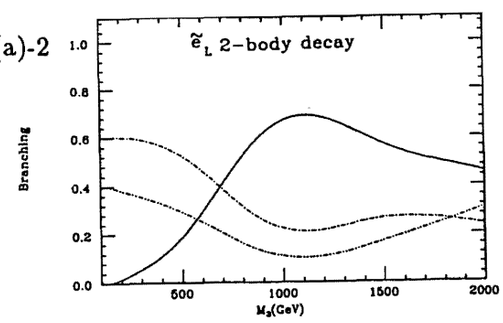

Fig.3(a)-1

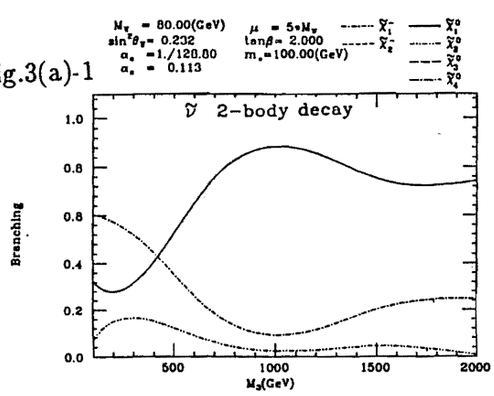

Fig.3(a)-3

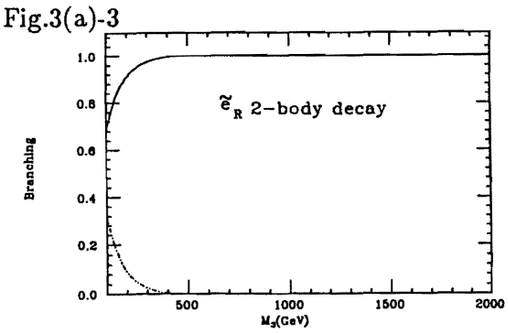

Fig.3(b)-1

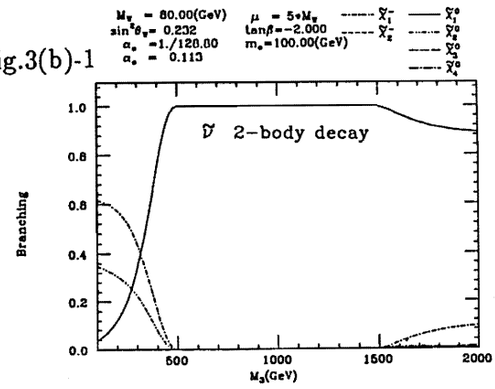

Fig.3(b)-2

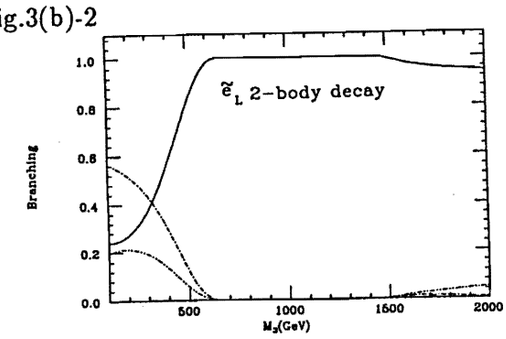

Fig.3(b)-3

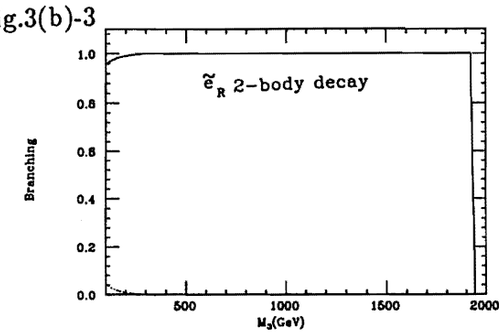

Fig.3(c)-1

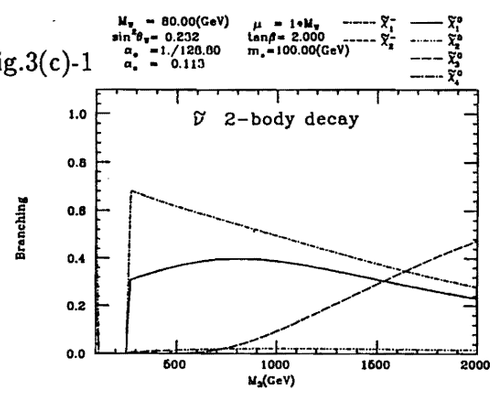

Fig.3(c)-2

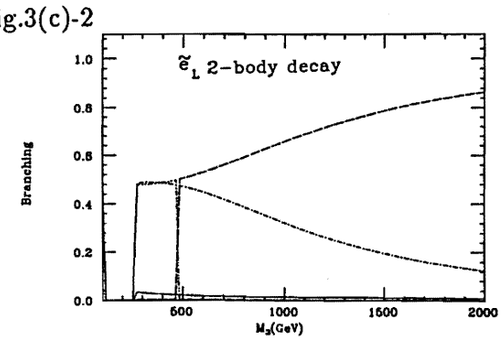

Fig.3(c)-3

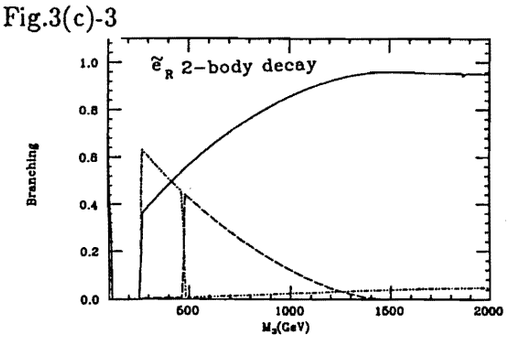

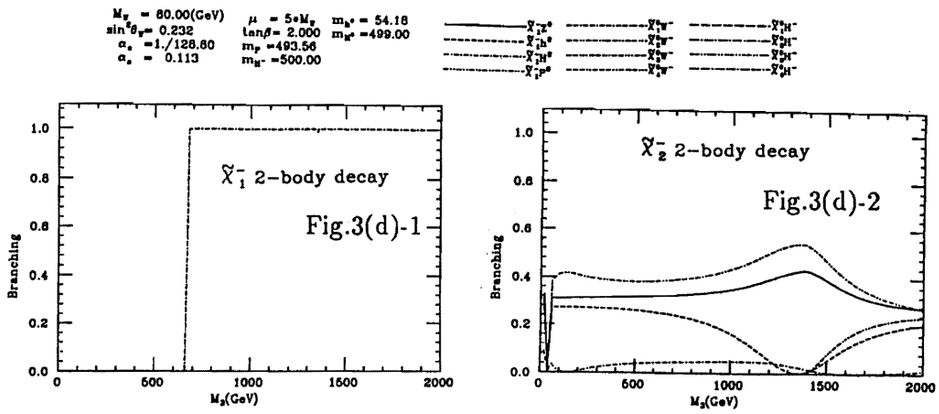
M_Z = 80.00(GeV)
$\sin^2\theta_W$= 0.232
α_s =1./128.60
α_s = 0.113
μ = 5*M_Z
tanβ= 2.000
m_P =493.56
m_{H^-} =500.00
m_{h^0} = 54.18
m_{H^0} =499.00
$\tilde{\chi}_1^-$ 2-body decay
Fig.3(d)-1
$\tilde{\chi}_2^-$ 2-body decay
Fig.3(d)-2
Branching
M_3(GeV)

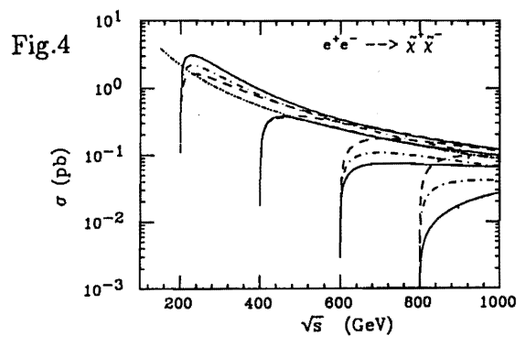
Fig.4
$e^+e^- \to \tilde{\chi}^+\tilde{\chi}^-$
σ (pb)
$\sqrt{s}$ (GeV)

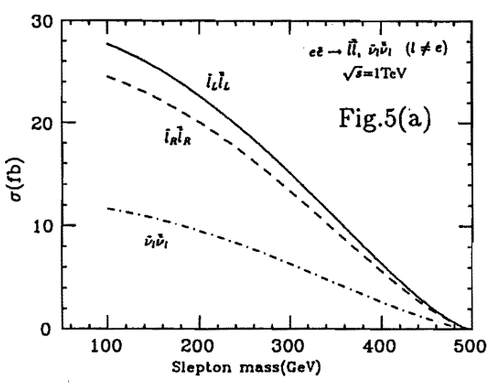
$e\bar{e} \to \tilde{l}\bar{\tilde{l}}$, $\tilde{\nu}_l\bar{\tilde{\nu}}_l$ ($l \neq e$)
$\sqrt{s}$=1TeV
Fig.5(a)
$\tilde{l}_L\bar{\tilde{l}}_L$
$\tilde{l}_R\bar{\tilde{l}}_R$
$\tilde{\nu}_l\bar{\tilde{\nu}}_l$
σ(fb)
Slepton mass(GeV)

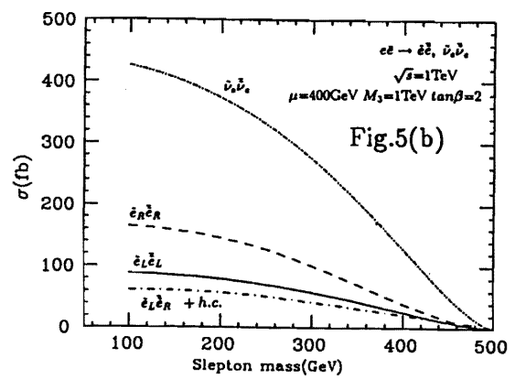
$e\bar{e} \to \tilde{e}\bar{\tilde{e}}$, $\tilde{\nu}_e\bar{\tilde{\nu}}_e$
$\sqrt{s}$=1TeV
μ=400GeV M_3=1TeV tanβ=2
Fig.5(b)
$\tilde{\nu}_e\bar{\tilde{\nu}}_e$
$\tilde{e}_R\bar{\tilde{e}}_R$
$\tilde{e}_L\bar{\tilde{e}}_L$
$\tilde{e}_L\bar{\tilde{e}}_R$ + h.c.
σ(fb)
Slepton mass(GeV)

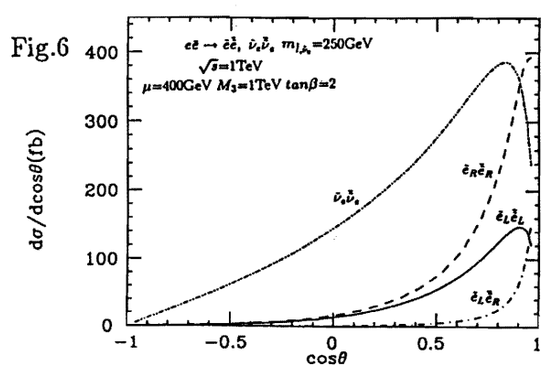
Fig.6
$e\bar{e} \to \tilde{e}\bar{\tilde{e}}$, $\tilde{\nu}_e\bar{\tilde{\nu}}_e$ $m_{l,\tilde{\nu}_e}$=250GeV
$\sqrt{s}$=1TeV
μ=400GeV M_3=1TeV tanβ=2
$\tilde{\nu}_e\bar{\tilde{\nu}}_e$
$\tilde{e}_R\bar{\tilde{e}}_R$
$\tilde{e}_L\bar{\tilde{e}}_L$
$\tilde{e}_L\bar{\tilde{e}}_R$
dσ/dcosθ(fb)
cosθ

Fig.7

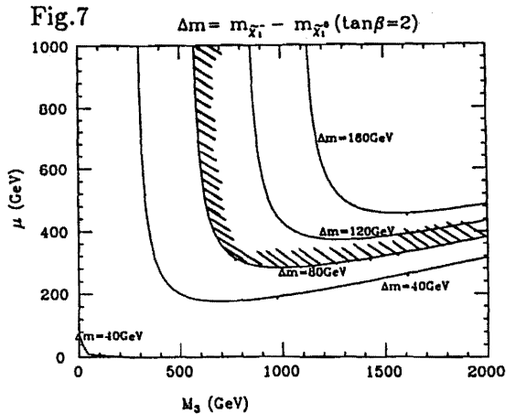

Fig.8(a)

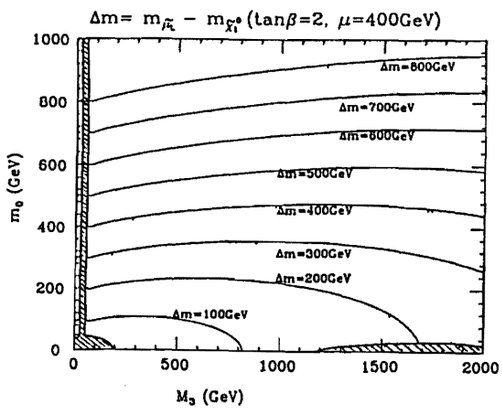

Fig.8(b)

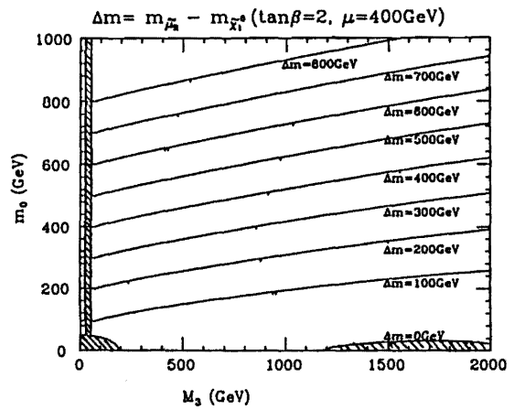

Fig.9(a)

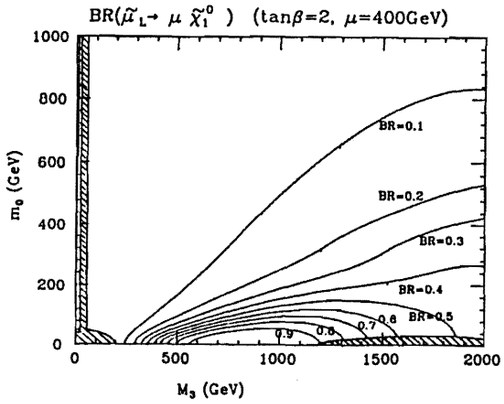

Fig.9(b)

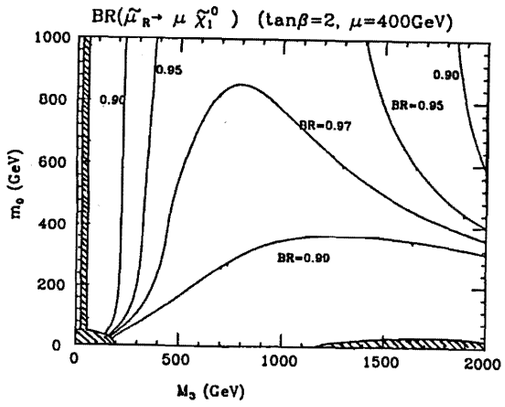

Fig.9(c)

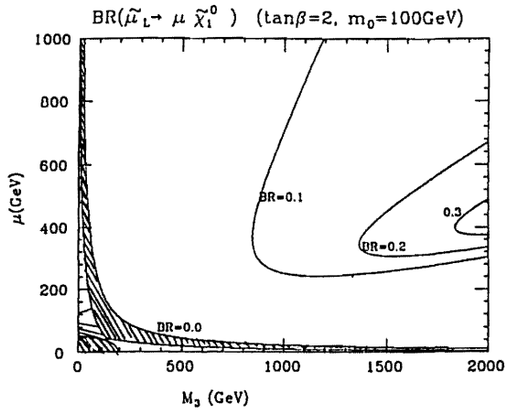

Fig.9(d)

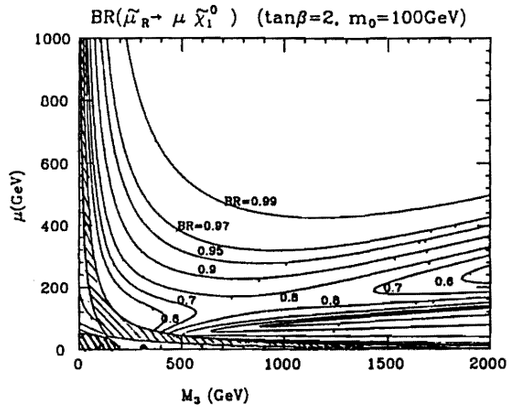

Fig.10(a)

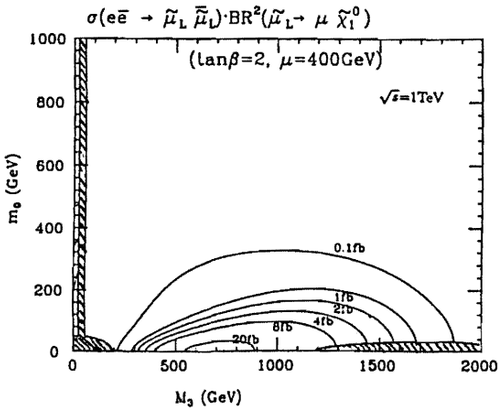
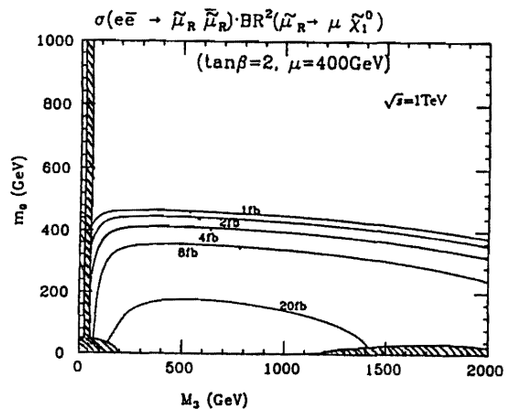
Fig.10(b)